Climate Dynamics (2003) 21: 221–232
DOI 10.1007/s00382-003-0332-6

M. M. Holland · C. M. Bitz

# Polar amplification of climate change in coupled models

Received: 21 November 2002 / Accepted: 11 March 2003 / Published online: 17 June 2003


**Abstract** The Northern Hemisphere polar amplification of climate change is documented in models taking part in the Coupled Model Intercomparison Project and in the new version of the Community Climate System Model. In particular, the magnitude, spatial distribution, and seasonality of the surface warming in the Arctic is examined and compared among the models. The range of simulated polar warming in the Arctic is from 1.5 to 4.5 times the global mean warming. While ice-albedo feedback is likely to account for much of the polar amplification, the strength of the feedback depends on numerous physical processes and parametrizations which differ considerably among the models. Nonetheless, the mean sea-ice state in the control (or present) climate is found to influence both the magnitude and spatial distribution of the high-latitude warming in the models. In particular, the latitude of the maximum warming is correlated inversely and significantly with sea-ice extent in the control climate. Additionally, models with relatively thin Arctic ice cover in the control climate tend to have higher polar amplification. An intercomparison of model results also shows that increases in poleward ocean heat transport at high latitudes and increases in polar cloud cover are significantly correlated to amplified Arctic warming. This suggests that these changes in the climate state may modify polar amplification. No significant correlation is found between polar amplification and the control climate continental ice and snow cover.

M. M. Holland (✉)
National Center for Atmospheric Research,
PO Box 3000, Boulder, CO 80307, USA
E-mail: mholland@ucar.edu

C. M. Bitz
Polar Science Center, Applied Physics Laboratory,
1013 NE 40th St, Seattle, WA 98105, USA

## 1 Introduction

Climate model simulations have shown that ice albedo feedbacks associated with variations in snow and sea-ice coverage are a key factor in positive feedback mechanisms which amplify climate change at high northern latitudes (e.g., Manabe and Stouffer 1980). In addition, variations in the thickness of sea-ice tend to reinforce surface atmospheric temperature anomalies by altering the heat and moisture transfer from the ocean to the atmosphere. Clouds respond to tropospheric temperature variations and most studies agree that clouds yield net positive radiative forcing at the surface in high latitudes (e.g., Curry et al. 1996). Hence, an increase in high-latititude cloud cover may also contribute to Northern Hemisphere polar amplification. High-latitude climate sensitivity also depends on changes in heat transported by the atmosphere and/or ocean.

There is agreement among models that the Arctic warms more than subpolar regions when subject to increasing levels of greenhouse gases (GHG) in the atmosphere. In contrast, high southern latitudes exhibit a minimum warming in coupled simulations due to changes in ocean heat uptake (IPCC 2001). At high latitudes in both hemispheres the range of warming across global climate models is considerable, with the range of warming in the Arctic being larger than elsewhere on Earth (IPCC 2001). Various physical processes and parametrizations lead to the wide range of high-latitude climate sensitivity in the models. A number of these processes appears to depend to some extent on the model's basic (unperturbed) climate state. For example, thin ice is more vulnerable to melting away due to anomalous warming, and hence a model whose sea-ice is biased towards being thin might be more sensitive to GHG forcing. The simulation of cloud cover during summer months is another consideration, because clouds can modify the surface radiation flux and hence the state of the surface ice cover. This influences the surface albedo leading to an

interdependency between cloud-radiation and ice-albedo feedbacks. Here we document the Northern Hemisphere polar amplification of surface warming in a group of coupled atmosphere–ocean–sea ice-land models that have been forced with increasing GHG levels. Because the control (present-day) climate conditions can influence feedbacks in the system, we also evaluate the dependence of the northern high-latitude warming on the basic simulated state of the sea-ice, snow coverage on land, and cloudiness. This gives some indication as to how biases in present-day simulations influence simulated high-latitude climate change.

Ingram et al. (1989) and Rind et al. (1995) investigated the influence of sea-ice conditions on climate sensitivity using an atmospheric general circulation model (AGCM) coupled to a simple sea-ice and slab ocean model. They found that feedbacks associated with changes in the sea-ice cover accounted for 20–40% of the global temperature change under $CO_2$ doubling conditions. While the Arctic was most sensitive, even the tropics warmed less in the absence of feedbacks from sea-ice, due to changes in heat transported by the atmosphere. Rind et al. (1995) determined that the sea-ice thickness and extent in the control simulations of the model were important for modifying the climate response to changes in atmospheric $CO_2$. In particular, thinner control climate ice-cover resulted in amplified warming at $2\times CO_2$ because it was more easily melted away as the climate warmed. A similar increase in climate sensitivity occurred with extensive control climate ice conditions, because larger sea-ice reductions were possible. In a further paper, Rind et al. (1997) also found that climate sensitivity depended more on ice thickness than on ice extent from the control climate in the Northern Hemisphere.

The influence of sea-ice conditions on climate sensitivity is further complicated in coupled models by an interactive ocean component. Changes in ocean dynamics and heat transport under increased greenhouse gases can modify the sea-ice response and hence the ice-albedo feedback mechanism. Changes in the ocean thermohaline circulation (THC) under climate change conditions are a well documented feature of climate models (e.g., IPCC 2001). However, the response of the THC varies considerably among models. Because this circulation is instrumental in transporting warm water to ice covered regions, changes in its strength can lead to a considerably different sea-ice response. This was recently discussed by Meehl et al. (2000a) in the comparison of two different climate models.

## 2 Model simulations

In this study, we analyze integrations from the second generation of models submitted to the Coupled Model Intercomparison Project (CMIP2), which include a control (or present-day) integration and an integration with a 1% per year compound increase in atmospheric $CO_2$ concentrations for each model. Each integration was run for at least 80 years. The activities and simulations performed for CMIP are discussed in Meehl et al. (2000b). Additionally, we analyze simulations (control and 1% increasing $CO_2$) from the Community Climate System Model Version 2 (CCSM2) which has just recently been released. All of the models used in this study are shown in Table 1. Also included in this table are the model representations of sea-ice. Although the sea-ice physics are not directly discussed, Table 1 gives some indication of the range of physical parametrizations that are used to represent the Arctic system. Several of the models participating in CMIP2 were not included here because they do not use an interactive ocean or sea-ice component, and hence all the models we include are fully coupled atmosphere–ocean–sea ice-land models. We focus on polar amplification in the model simulations, which is primarily limited to the Northern Hemisphere in models subject to a transient increase in $CO_2$ level (IPCC 2001).

## 3 Polar amplification in the models

In the following analysis, we define the average conditions at the time when the atmospheric concentration of $CO_2$ reaches twice its present level (abbreviated as $2\times CO_2$) as the 20 year mean centered around the time of doubling (i.e., years 61–80). The values at $2\times CO_2$ are then subtracted from the 80 year average conditions from the control integrations to give a measure of change. The globally averaged 2 m air temperature change at $2\times CO_2$ for the models is shown in Table 2. The temperature change ranges from approximately 1–2 °C. The range of global temperature response results from different representations of feedback processes in the models, which may depend, in part, on the sea-ice and snow cover, and on the rate of ocean heat uptake.

To isolate polar amplification of the warming, we examine the change in zonally averaged 2 m air temperature normalized by the global mean air temperature change. This gives us a measure of how "amplified" the global warming signal is at high latitudes. For example, a normalized warming of 3, indicates that the warming is three times larger than the global average. Figure 1 shows the normalized increase in the zonally averaged 2 m air temperature as a function of latitude for the $2\times CO_2$ conditions. All of the simulations show amplified warming at high northern latitudes, with warming from 75–90°N that is typically between two and three times the global average. Six of the models have considerably larger polar amplification; over three times the global warming signal. We identify these six models as having "high" polar amplification using this somewhat arbitrary cutoff. The models that meet this criteria are the CCC, GISS, MRI, CCSM2, CCSR, and BMRC. We define the polar amplification in the remaining models as "low to moderate". As seen from Table 2, high polar amplification is unrelated to the global temperature change in the simulations.

A feature that is apparent from Fig. 1 is that the maximum warming in the different simulations does not always occur at the highest northern latitudes. The difference in spatial distribution of the warming is

**Table 1** Models used in this study

| Group | Reference | Abbreviation | Sea-ice physics |
|---|---|---|---|
| Bureau of Meteorology Research Center (Australia) | Power et al. (1998); Colman (2001) | BMRC | Th, no leads |
| Canadian Centre for Climate Modelling and Analysis (Canada) | Flato et al. (2000) | CCC | Th, leads |
| Center for Climate System Research (Japan) | Emori et al. (1999) | CCSR | Th, no leads |
| Centre Europeen de Recherche et de Formation Avancee en Calcul Scientifique (France) | Barthelet et al. (1998a, b) | CERF | Th, statistical ITD |
| Commonwealth Scientific and Industrial Research Organization (Australia) | Gordon and O'Farrell (1997) | CSIR | Th, CF dyn, leads |
| Max-Planck-Institut fuer Meteorologie (ECHAM3 + LSG Model) (Germany) | Cubasch et al. (1997) | ECH3 | Th, no leads |
| Geophysical Fluid Dynamics Laboratory (R15 Model) (USA) | Manabe et al. (1991) | GFDL-A | Th, free drift |
| Geophysical Fluid Dynamics Laboratory (R30 Model) (USA) | Delworth and Knutson (2000) | GFDL-B | Th, free drift |
| Goddard Institute for Space Studies (Russell Model) (USA) | Russell et al. (1995) | GISS | Th, leads |
| Meteorological Research Institute (Japan) | Tokioka et al. (1996) | MRI | Th, free drift |
| National Center for Atmospheric Research (CSM Model) (USA) | Boville and Gent (1998) | CSM | Th, CF dyn, leads |
| Department of Energy (Parallel Climate Model) (USA) | Washington et al. (2000) | PCM | Th, EVP dyn, leads |
| United Kingdom Meteorological Office (HadCM2 Model) (UK) | Johns (1996) | UKMO2 | Th, free drift, leads |
| United Kingdom Meteorological Office (HadCM3 Model) (UK) | Gordon et al. (2000) | UKMO3 | Th, free drift, leads |
| National Center for Atmospheric Research (CCSM2 Model) (USA) | Kiehl and Gent (2002), in preparation | CCSM2 | Th, EVP dyn, leads, ITD |

Th indicates thermodynamic models, ITD denotes the inclusion of a subgridscale ice thickness distribution, CF dyn refers to dynamics with a cavitating fluid rheology (Flato and Hibler 1992), EVP dyn refers to dynamics with an elastic-viscous-plastic rheology (Hunke and Dukowicz 1997), and free drift refers to the use of a free drift approximation which neglects the internal ice pressure

**Table 2** The change in global average 2 m air temperature at $2\times CO_2$. The models with "high" polar amplification are shown in bold

| Group | Temperature change (°C) |
|---|---|
| **CCSM2** | **1.08** |
| PCM | 1.31 |
| CSM | 1.44 |
| **GISS** | **1.44** |
| ECH3 | 1.58 |
| **BMRC** | **1.58** |
| **MRI** | **1.60** |
| **CCSR** | **1.62** |
| CERF | 1.64 |
| UKMO2 | 1.75 |
| GFDL-A | 1.89 |
| **CCC** | **1.92** |
| **CSIR** | 2.00 |
| UKMO3 | 2.04 |
| GFDL-B | 2.15 |

more prominent in Fig. 2 which shows maps of the normalized temperature change at $CO_2$ doubling. The location of the maximum warming varies widely among the models. However, the models can be separated into those that have a maximum warming over the Arctic basin (e.g., CCC, GISS, MRI, BMRC, CCSM2, CCSR, CERF, GFDL-B, GFDL-A, ECH3) and those that have a maximum warming along the ice edge (e.g., UKMO2, UKMO3, CSIR, PCM, and CSM). The six models with high polar amplification generally have the maximum warming signature over the Arctic basin, although the CCSM2 warming is shifted towards the Kara Sea. In the PCM and CSM models, the maximum warming is quite large but is located relatively far south, along the Greenland coast. As we will show in the next section, the spatial distribution of the warming is closely related to the sea-ice conditions in the control simulation.

The temperature change at $2\times CO_2$ is shown as a function of latitude and month in Fig. 3. We again see a number of features of the high-latitude warming that are present in the other figures. In particular, all the simulations have amplified Arctic warming and the latitude at which the maximum warming occurs varies considerably among the models. In addition, we can see from this figure the variation in time of year at which the maximum warming occurs. All of the models warm the least (near zero) during the summer months. This has been discussed previously (e.g., IPCC 1995) and results from the fact that the surface temperature remains close to the melting temperature under $2\times CO_2$ conditions due to the presence of sea-ice or, in simulations with ice-free Arctic summers, due to the thermal inertia of the ocean mixed layer. The month of maximum warming varies from October to March among the simulations.

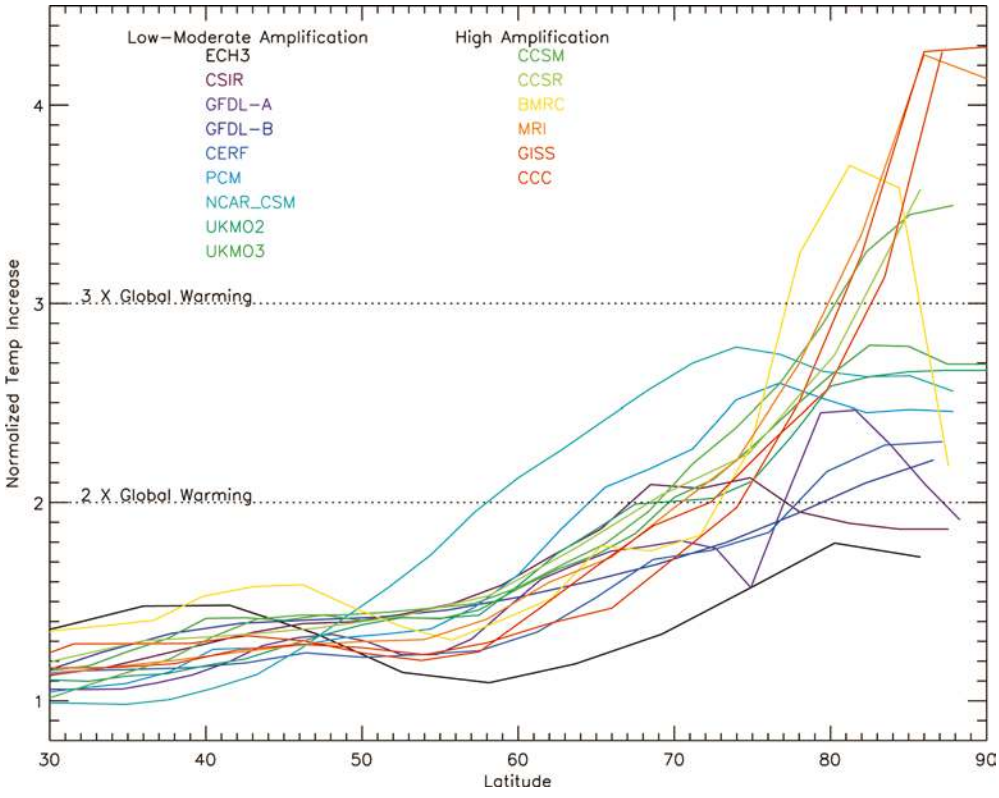


**Fig. 1** The increase in zonally averaged 2 m air temperature for $2\times CO_2$ conditions as a function of latitude normalized by the globally averaged air temperature increase

## 4 Relationship of the polar amplification signals to the state of the sea ice, snow coverage on land, cloudiness, and ocean heat transport

The models discussed here have numerous differences in their physical components making it difficult to attribute the changes in polar amplification to any one physical mechanisms. However, we do find that the control climate basic state, particularly that of the sea-ice, modifies the high-latitude climate response.

### 4.1 Sea ice

The models discussed in this study have a considerable range in the present-day simulation of sea-ice conditions. Figure 4 shows the mean sea-ice thickness and extent simulated by the models for the control climate. The annual average ice extent ranges from $8 \times 10^6$ km$^2$ to over $20 \times 10^6$ km$^2$ and the mean ice thickness from 0.3 m to 2.5 m. Additionally, the spatial distribution of ice thickness across the basin varies considerably. For a further discussion of control and perturbed climate sea ice conditions in the CMIP models, the reader is referred to Flato (2003 submitted). Sea-ice simulations in individual models have also been discussed in a number of papers for both control climate and climate change integrations. In addition to some of the references shown in Table 1, these include studies by Johns et al. (1997) (UKMO2), O'Farrell (1998) (CSIR), Weatherly et al. (1998) (NCAR_CSM), and Weatherly and Zhang (2001) (PCM).

Figure 5 shows a plot of the latitude at which maximum warming occurs versus the ice extent for the 15 models discussed in this study. Ice extent is defined as the total area in the Northern Hemisphere where the sea-ice is thicker than 10 cm. Therefore, the area of leads is included in the ice extent provided the mean thickness in the region (i.e., grid cell) is at least 10 cm. The ice extent and latitude of maximum warming are significantly correlated at the 99% level at $R = -0.80$. This indicates a general tendency for models with larger ice extents to obtain their maximum warming further south. Because these models have more southerly ice extents, they exhibit more southerly changes in ice cover and albedo, resulting in a larger simulated temperature response at these latitudes.

Plots of sea-ice conditions versus the maximum zonally averaged normalized temperature change are shown in Fig. 6. Rind et al. (1995) looked at global warming as a function of sea-ice extent in the GISS model (although not the same GISS model that participated in CMIP2) and found higher global sensitivity resulted when ice extent is larger in the present climate because there is more sea-ice available to lose. We find the same is true for the polar amplification in the coupled models considered here *only* for models with low to moderate ($< 3$) polar amplification. Figure 6a shows that the maximum warming increases weakly with increasing ice extent among these models, with a correlation coefficient of $R = 0.65$ which is significant at the 95% level. For these

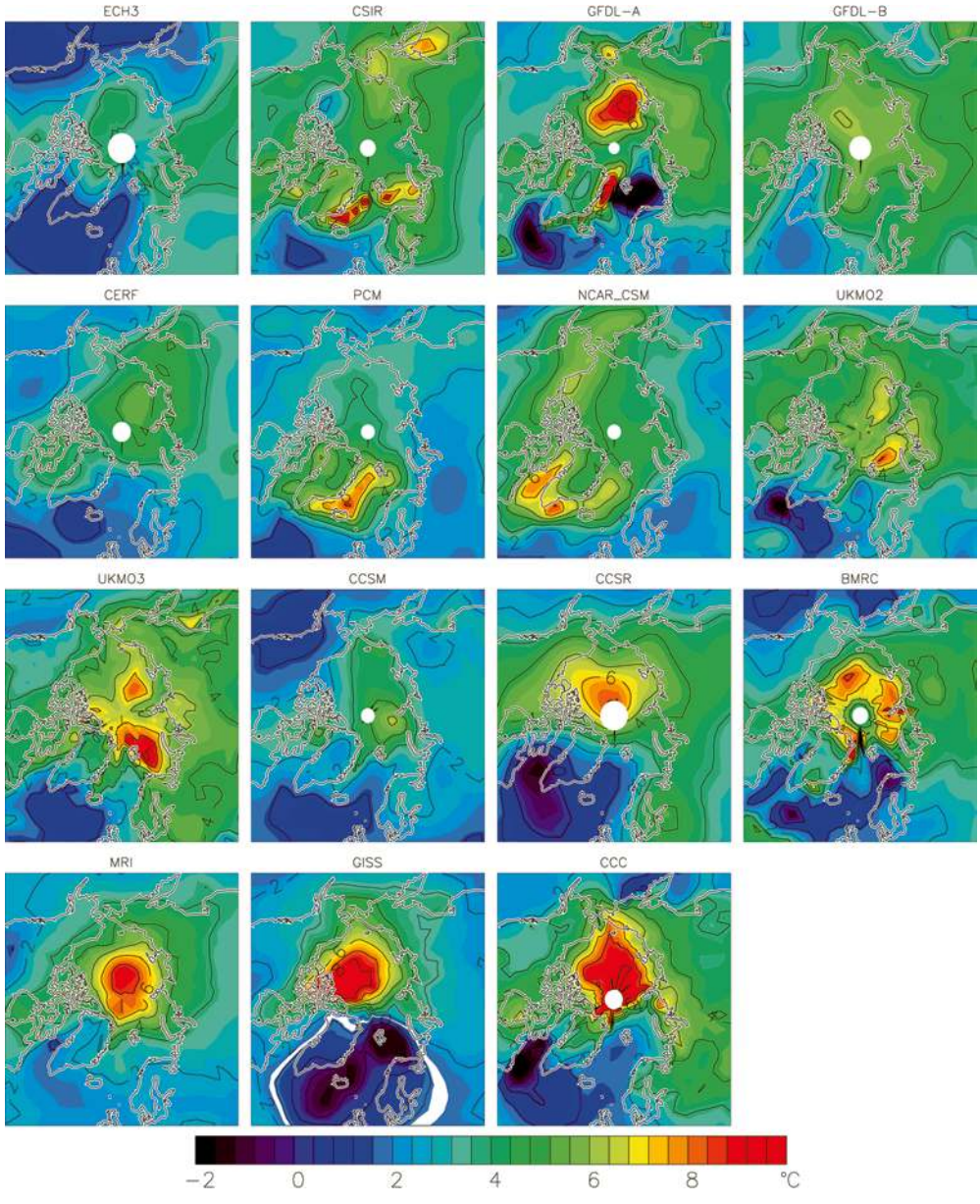


**Fig. 2** The temperature change for 2×$CO_2$ conditions normalized by the global average air temperature change

models there is also a significant correlation between the control climate ice extent and the change in ice extent at 2×$CO_2$ conditions. However if we consider all the models together, we find no significant correlation between ice extent and normalized warming.

Figure 6b shows a scatter plot of the control climate ice thickness versus the polar amplification. In the coupled models considered here, we find that polar amplification is more highly correlated (albeit still weak) to the sea-ice thickness than to the ice extent. When all models are considered together, the correlation is $R = -0.40$, which is significant at the 93% level. As will be shown later, the GISS and MRI models show an anomalous increase in poleward ocean heat transport at 2×$CO_2$ conditions and the GISS model shows an anomalous increase in winter polar cloud cover. This may influence the polar amplification in these models. If we remove them from the analysis, then the amplitude of the correlation between control climate ice thickness and polar amplification increases to a value of $R = -0.66$ which is significant at the 99% level. Models with thin control climate ice cover typically have larger changes in ice extent at 2×$CO_2$ conditions. Whether this is a cause of, or results from, the amplified warming in these integrations is not clear from the data available for the model simulations. However, it does suggest the possibility that models with thinner ice cover have enhanced ice extent loss because the thin ice is more easily melted away. This in turn would result in a larger albedo feedback and loss of insulation between ocean and atmosphere and would amplify the high northern latitude warming.

Among the CMIP models, the control climate sea-ice conditions appear to modify the polar amplification in

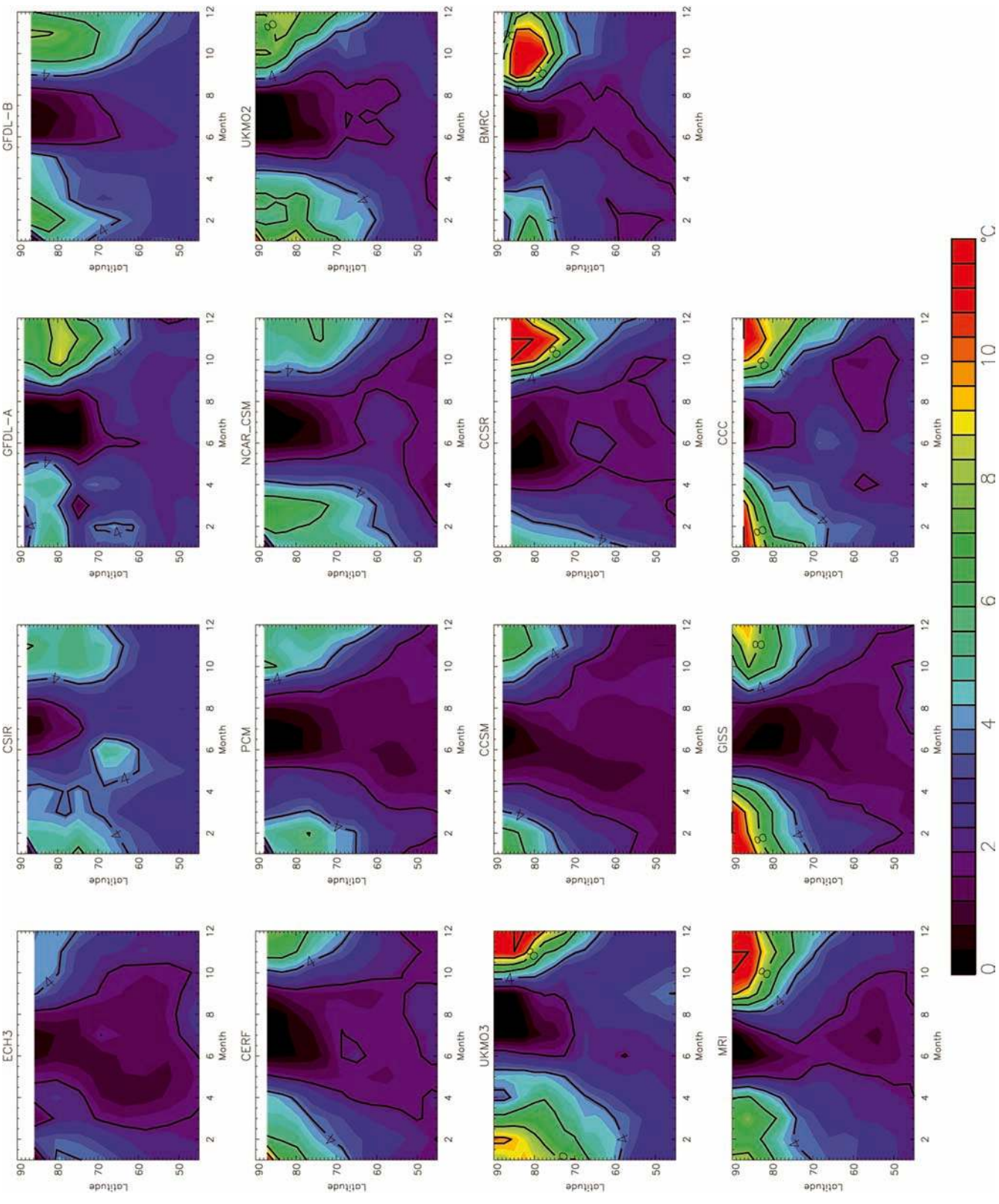


**Fig. 3** The change in 2 m air temperature at $2\times CO_2$ as a function of month and latitude

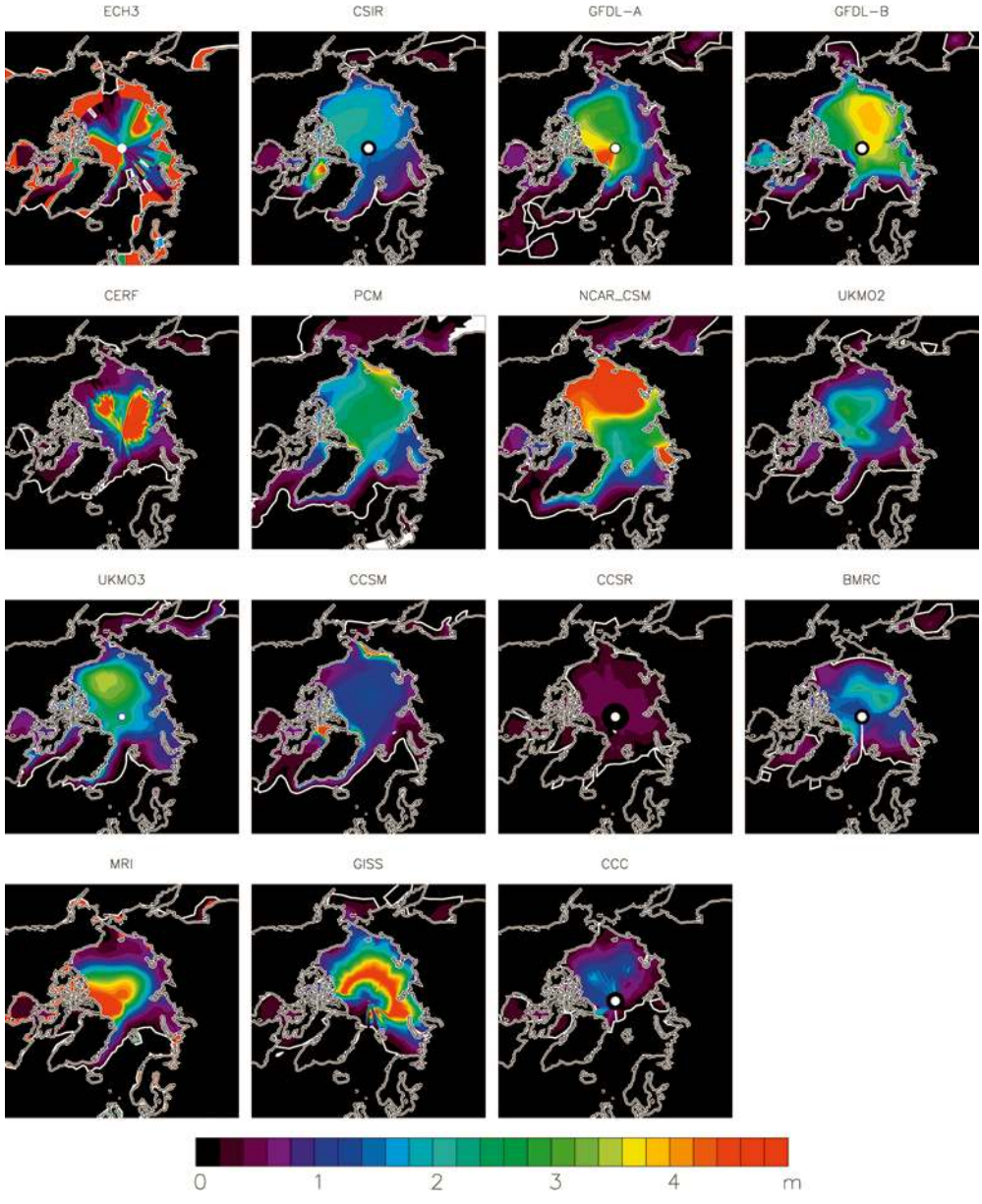


**Fig. 4** The ice thickness and extent in the model simulations

the Northern Hemisphere. However, the different sensitivity to control climate ice extent for models with high and low-moderate amplification and the somewhat weak correlation between control climate ice thickness and polar amplification when all models are considered, suggests that other processes, such as changes in ocean heat transport, may influence the high latitude response to increasing $CO_2$. Later we consider three alternative conditions in the models to determine further cause for the range of polar amplification seen across the CMIP simulations.

## 4.2 Snow coverage on land

We examine the relationship between polar amplification and snow coverage on land, for the same reason as was done for sea ice, with the expectation that when snow extent is larger in the present climate there is more snow available to lose and hence a stronger albedo feedback will be present. Figure 7 shows the Northern Hemisphere snow extent on land versus the polar amplification in the models. When all models are considered, there is no significant correlation between the snow extent in the control climate and the simulated polar amplification ($R < 0.01$). However, when only the models with moderate-to-low polar amplification are considered, a significant correlation exists between snow extent and the amplified warming ($R = 0.67$, which is significant at the 95% level). Thus we find polar amplification is weakly related to snow extent, in a similar fashion to the way it is related to sea-ice extent. Furthermore we find the extent of sea-ice and snow on land are significantly correlated at the 95% level ($R = 0.54$)

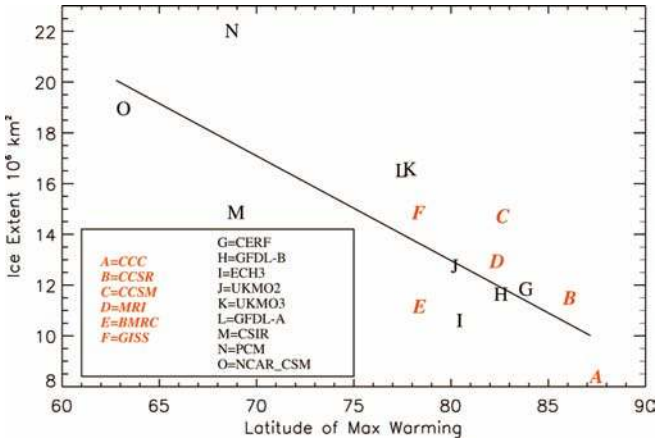


**Fig. 5** Scatter plot of the Northern Hemisphere control climate ice extent (in $10^6$ km$^2$) versus the latitude of maximum warming at $2\times CO_2$. The models with high polar amplification are shown in red

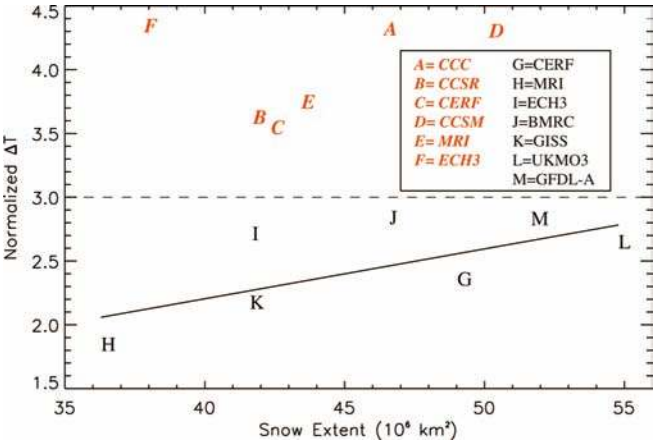


**Fig. 7** Scatter plot of the control climate Northern Hemisphere snow extent (in $10^6$ km$^2$) versus the maximum zonally averaged 2 m normalized air temperature. The snow extent was calculated as the area where the snow depth exceeded 10% of the model's mean and this mean excludes regions where snow depths exceed 10 times the median to eliminate ice sheets such as Greenland. The models with high polar amplification are shown in *red*. The regression for models with low-to-moderate polar amplification is shown

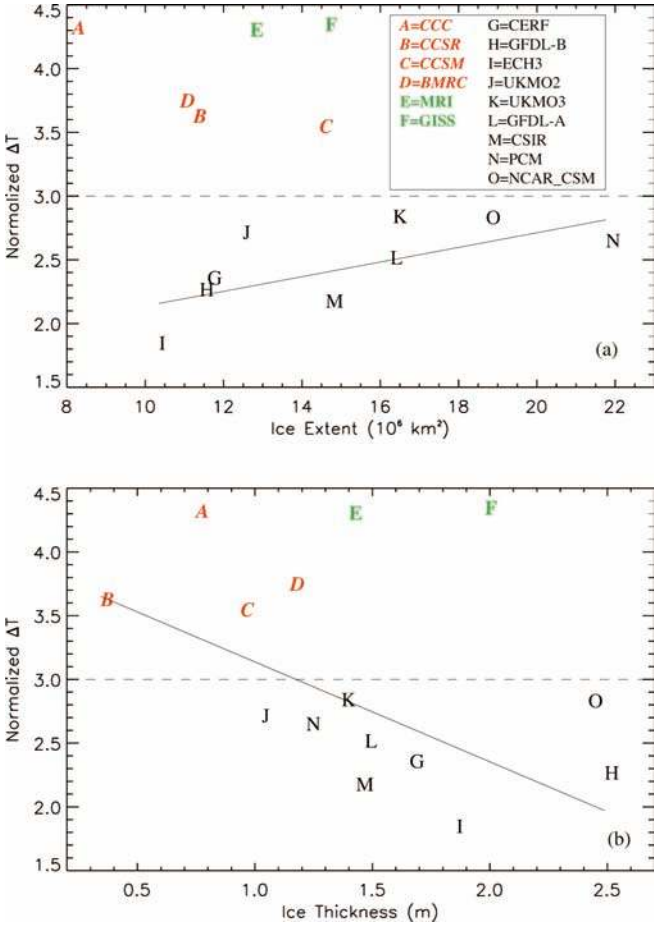


**Fig. 6** Scatter plots of **a** control climate ice extent (in $10^6$ km$^2$) versus the maximum zonally averaged 2 m normalized air temperature and **b** control climate ice thickness (in m) versus the maximum zonally averaged 2 m normalized air temperature for the northern hemisphere. In **a**, the regression for models with low-to-moderate polar amplification is shown. In **b**, the regression for all models except the two most extreme outliers (*E* and *F*) is shown

in the control climate simulations, making it difficult to know which, if either, has a fundamental influence on climate sensitivity in models with moderate-to-low polar amplification.

If the extent of the snow coverage influenced the strength of albedo feedback over land, we would expect a significant correlation between the control climate snow extent and the decrease in snow cover. However, there is no significant correlation between these variables when all the models are considered or when only the models with low-to-moderate amplification are considered. Based on this analysis, it appears that the snow coverage on land in the control climate has little influence on the simulated Northern Hemisphere polar amplification. Instead, it is likely that the significant correlation which results for the low-to-moderate models is a consequence of the relationship between ice extent and snow cover.

### 4.3 Cloud coverage

We consider how cloud cover contributes to polar amplification in these simulations. It is often said that clouds reduce the strength of the ice-albedo feedback by shielding the planetary albedo from the surface (e.g., Shine et al. 1984; Ingram et al. 1989). Furthermore most models predict Arctic cloud cover increases with warming (e.g., Wetherald and Manabe 1988), which increases the planetary albedo and reduces downward shortwave radiation at the surface. This may reduce the polar warming although Washington and Meehl (1996) found the surface albedo changes due to reductions in sea-ice cover still dominate the climate response at high latitudes. In contrast, higher cloud cover increases the downward longwave radiation at the surface which may

**Table 3** Summertime cloud coverage in the control climate and the increase at $2\times CO_2$ averaged north of 70 degrees for April–September (except GISS which is March–August)

| Group | Control climate cloud coverage | Cloud coverage increase |
|---|---|---|
| **CCC** | **45.6%** | **3.3%** |
| GFDL-A | 47.3% | 0.7% |
| UKMO3 | 60.2% | 2.1% |
| CSIR | 64.9% | 0.9% |
| UKMO2 | 70.4% | 1.3% |
| **GISS** | **72.0%** | **3.4%** |
| PCM | 75.0% | 0.8% |
| **CCSM2** | **75.7%** | **–0.2%** |
| CSM | 78.2% | 0.4% |

**Table 4** Wintertime cloud coverage in the control climate and the change at $2\times CO_2$ averaged north of 70 degrees for October–March (except GISS which is September–February)

| Group | Control climate cloud coverage | cloud coverage change |
|---|---|---|
| GFDL-A | 46.6% | 3.3% |
| **CCC** | **50.3%** | **4.3%** |
| **GISS** | **57.7%** | **10.1%** |
| UKMO3 | 62.2% | –1.1% |
| UKMO2 | 79.6% | 1.8% |
| **CCSM2** | **81.1%** | **–0.8%** |
| PCM | 87.9% | –1.8% |
| CSM | 89.3% | –1.6% |
| CSIR | 91.5% | –4.2% |

enhance the polar warming. This process can be particularly effective in the winter, when there are no compensating changes in the solar radiation at the surface.

The control climate cloud cover during summer (April–September) and its increase at $2\times CO_2$ is shown in Table 3. We were only able to acquire cloudiness data from nine of the models we analyzed, and among those nine the correlation between polar amplification and control climate summer cloud coverage is weak ($R$ = –0.11). This indicates that there is not a robust relationship between the basic state of the Arctic summer cloud cover and polar amplification in these models, and there is no evidence of clouds shielding the ice-albedo feedback at the surface. We found essentially no correlation between the change in absorbed solar radiation at the surface and the change in cloud cover ($R$ = 0.01), suggesting that surface albedo changes far outweigh the influence of cloud changes on the surface shortwave radiation budget.

Simulations with higher polar amplification do generally exhibit a larger increase in summer cloud cover, with the two significantly correlated (at the 98% level) at $R$ = 0.68. An increase in cloud cover would reduce the amount of shortwave radiation incident on the surface, which in turn may reduce the surface warming and polar amplification. However, increasing clouds also increase the surface downward longwave flux. The positive correlation between polar amplification and cloud cover changes indicates that either the net cloud radiative forcing is positive and that clouds act as a positive feedback or that clouds are simply responding to the warming.

In order to elucidate whether surface longwave changes associated with changing cloud cover may influence the simulated polar amplification, we examine cloud coverage in winter (October–March), when solar radiation is absent. The results presented in Table 4 show that models with low winter cloud cover in the control climate tend to have higher polar amplification ($R$ = –0.50, which is significant at the 92% level). Additionally, the control climate cloud conditions during winter are related to the change in winter clouds at $2\times CO_2$ conditions, with the two correlated at $R$ = –0.76 which is significant at the 99% level. The changes in cloud cover are in turn correlated to the simulated polar amplification, and models with larger winter cloud cover changes experience higher polar amplification ($R$ = 0.74, significant at the 99% level). It is possible that the winter polar clouds are simply responding to the polar warming. However, the relationships between polar amplification and winter cloud cover do suggest that changes in the downward surface longwave radiation associated with winter cloud cover changes are modifying the simulated polar amplification. Additionally, the GISS model, which obtains one of the largest polar amplification signals but has average sea-ice conditions, also exhibits the largest increase in winter cloud cover. The changes in winter cloud conditions also appear to be influenced by the control climate conditions with larger increases observed for models with lower present day cloud fractions.

### 4.4 Ocean heat transport

Changes in poleward ocean heat transport at high latitudes can modify the sea-ice retreat under climate change scenarios and also the heat available to the atmosphere. There is evidence that these changes are important for the high-latitude warming in the models considered here. For example, in Fig. 2, there are a number of models that show a region of reduced warming or even cooling over the high-latitude North Atlantic. This results from a reduction in the ocean thermohaline circulation and a reduced heat transport into these regions.

Ocean heat transport data were available and examined for eight of the coupled models. Figure 8a shows the change in poleward ocean heat transport at $2\times CO_2$ from 40–90°N for the models with available data. There is a considerable range in the simulated response. The polar amplification is significantly correlated to both the control climate ocean heat transport and the change in transport simulated by the model at high latitudes (Fig. 8b). Additionally, the change in heat transport at high latitudes is significantly correlated to both the decrease in ice extent and the decrease in ice thickness poleward of 70°N. Although this correlation does not

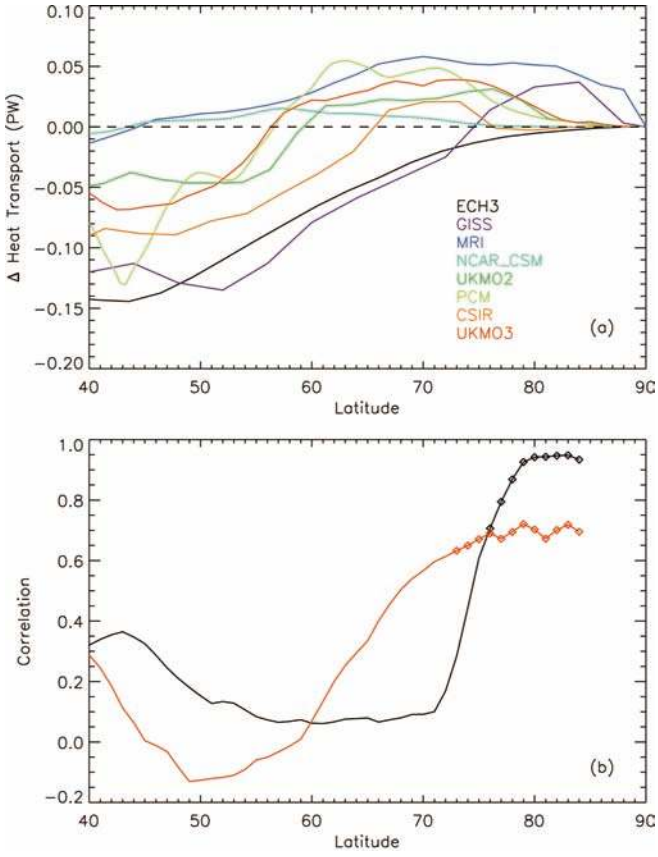


**Fig. 8** **a** The change in poleward ocean heat transport at $2\times CO_2$ conditions as a function of latitude for the models with available data. **b** Correlation of the control climate ocean heat transport (*red line*) and the change in ocean heat transport (*black line*) with the maximum zonally averaged 2 m normalized air temperature for the Northern Hemisphere. Values that exceed the 95% significance level are shown by *diamonds*

necessarily indicate a causal relationship between ocean heat transport and ice conditions, it does suggest the possibility that increased ocean heat transport results in thinner and less extensive Arctic ice cover. This in turn would enhance the surface albedo feedback and enhance the polar amplification. More studies, including sensitivity tests with a single model are needed to further investigate this finding.

The MRI simulation has enhanced transport everywhere north of 45°N and has the largest increase in northward heat transport for the high latitudes. This may contribute to the enhanced polar warming in this model even in light of its relatively thick ice cover. Additionally, although the GISS model has a large decrease in poleward ocean heat transport south of 75°N, it does obtain a relatively high increase in heat transport north of this latitude. Thus, it is possible that even though the reduced transport south of 75°N results in colder temperatures in the Nordic Seas, the enhanced transport into the Arctic basin contributes to a decrease in ice thickness and amplifies the albedo feedback.

## 5 Conclusions and discussion

We have documented the $2\times CO_2$ warming at high northern latitudes as seen in models participating in the coupled model intercomparison project 2 (CMIP2) and in the CCSM2. As seen in previous studies, all of the models simulate amplified warming at high northern latitudes. We isolated the models' polar amplification by normalizing the change in 2 m air temperature by its global mean. Using this measure, the polar amplification varies considerably between the model simulations. Models with the lowest amplification have zonally averaged temperature increases at $2\times CO_2$ conditions that are less than twice the global average temperature change. Models with the highest polar amplification exhibit zonally averaged temperature increases that are greater than four times the globally averaged values. The majority of the models simulate maximum zonally averaged polar warming that is 2–3 times the globally averaged value. Both the location and month of maximum warming vary considerably among the simulations, with the maximum warming occurring between October and March.

Our results show that several aspects of polar amplification in the Arctic are related to the control climate sea-ice conditions. For example, the spatial distribution of the warming is affected by the simulated present-day ice conditions. In particular, ice extent is significantly correlated with the latitude of maximum warming and models with larger ice extent generally exhibit larger warming further south. This results from local positive feedback processes that occur in regions of ice retreat.

Additionally, the magnitude of the polar amplification is related to the control climate sea-ice conditions. There is a significant correlation between the control climate ice thickness and polar amplification, in that simulations with thinner ice cover obtain higher polar amplification. In four out of six of the models that exhibit "high" polar amplification, thin ice cover is present in the control simulation, indicating that this contributes to the enhanced polar warming. As discussed by Rind et al. (1995), the presence of thin ice cover can increase the model sensitivity, because this ice is more easily melted away, resulting in a stronger surface albedo feedback mechanism. The other two models with high polar amplification have moderate to thick sea-ice, indicating that conditions other than the sea-ice basic state are influencing the high-latitude climate response. In these models, there is evidence that this is associated with changes in ocean heat transport or polar cloud cover. Additionally, parametrizations of the ice cover, such as the representation of lateral melting, are also possible culprits for the different high latitude sensitivity in these models.

For models with low-to-moderate ($<3$ normalized warming) polar amplification, there is a tendency for higher polar amplification to occur in models with larger

control climate ice extent. This agrees qualitatively with the atmospheric GCM results of Rind et al. (1995) and appears to result from the fact that in models with larger ice extents, there is more ice available to lose and hence larger positive sea-ice feedbacks result. The apparent different behavior with respect to ice extent in models with high polar amplification, suggests that a different sensitivity to ice extent is likely depending on the other sea-ice conditions, such as its thickness.

Snow cover extent over land is significantly correlated to the control climate sea-ice extent. As occurs for the ice cover, the control climate snow extent is significantly correlated to polar amplification for models with low-to-moderate polar amplification. However, there is no correlation between the control climate snow cover and the decrease in snow extent at $2\times CO_2$ conditions, suggesting that the correlation between control climate snow cover and polar amplification is a consequence of the tendency for simulations with higher ice extent to also have higher snow extent.

Polar cloud cover was also examined to determine its influence on the simulated polar amplification. No significant relationship was found between the polar amplification and control climate cloud cover during the summer. However, models with low control climate winter cloud cover tended to have higher polar amplification and a larger increase in cloud fraction at $2\times CO_2$ conditions. Additionally, the polar warming was positively and significantly correlated to the increase in both summer and winter cloud cover. Although clouds may be simply responding to the amplified warming, it is also possible that clouds act as a positive feedback at high latitudes by increasing the downward longwave radiation at the surface.

Models with higher polar amplification were also shown to have a tendency for both enhanced control climate ocean heat transport and larger changes in ocean heat transport at high northern latitudes (poleward of approximately 75°N). Thus, it appears possible that changes in ocean circulation at high latitudes are modifying the polar amplification in these models. As for the other climate conditions considered here, further studies using, for example, sensitivity simulations within a single model are needed to elucidate and quantify the relationships that have been suggested by the model intercomparison presented here.

Because the models examined here differ in numerous aspects, it is difficult to attribute the various polar amplification signals to any single property or process in the model. However, our discussion does indicate that the control climate sea-ice conditions are important for determining the magnitude and spatial distribution of the northern high latitude warming. Climate models are being used increasingly to examine the regional effects of climate change. This study suggests that realistically simulating the control climate sea-ice conditions is important if we are to accurately represent the regional Arctic response to increasing greenhouse gases.

**Acknowledgements** We gratefully acknowledge the CMIP modeling groups for conducting the CMIP model simulations and making the model data available. The Program for Climate Model Diagnostics and Intercomparison (PCMDI) at the Lawrence Livermore National Laboratory is also acknowledged for archiving and providing the CMIP model data. We thank Dr. Peter Gent for comments on a draft manuscript and Dr. Greg Flato for useful discussions during the course of this work. We also thank two anonymous reviewers for helpful comments. This work was supported in part by a grant from the National Science Foundation, Office of Polar Programs through the SHEBA phase 3 program to MM Holland. CM Bitz was supported by NSF grant OPP0084287.

## References

Barthelet P, Bony S, Braconnot P, Braun A, Cariolle D, Cohen-Solal E, Dufresne J-L, Delecluse P, Deque M, Fairhead L, Filiberti M-A, Forichon M, Grandpeix J-Y, Guilyardi E, Houssais M-N, Imbard M, LeTreut H, Levy C, Li ZX, Madec G, Marquet P, Marti O, Planton S, Terray L, Thual O, Valcke S (1998a) Simulations couplees globales de changements climatiques associes a une augmentation de la teneur atmospherique en $CO_2$. CR Acad Sci Paris, Sciences de la terre et des planetes (in French with English summary) 326: 677–684

Barthelet P, Terray L, Valcke S (1998b) Transient $CO_2$ experiment using the ARPEGE/OPAICE nonflux corrected coupled model. Geophys Res Lett 25: 2277–2280

Boville BA, Gent PR (1998) The NCAR Climate System Model, Version One. J Clim 11: 1115–1130

Colman RA (2001) On the vertical extent of atmospheric feedbacks. Clim Dyn 17: 391–405

Cubasch U, Voss R, Hegerl GC, Waszkewitz J, Crowley TJ (1997) Simulation of the influence of solar radiation variations on the global climate with an ocean–atmosphere general circulation model. Clim Dyn 13: 757–767

Curry JA, Rossow WB, Randall D, Schramm JL (1996) Overview of Arctic cloud and radiation characteristics. J Clim 9: 1731–1764

Delworth TL, Knutson TR (2000) Simulation of early 20th century global warming. Science 287(5461): 2246–2250

Emori S, Nozawa T, Abe-Ouchi A, Numaguti A, Kimoto M, Nakajima T (1999) Coupled ocean–atmosphere model experiments of future climate change with an explicit representation of sulfate aerosol scattering. J Metorol Soc Japan 77: 1299–1307

Flato GM, Boer GJ, Lee WG, McFarlane NA, Ramsden D, Reader MC, Weaver AJ (2000) The Canadian Centre for Climate Modelling and Analysis global coupled model and its climate. Clim Dyn 16: 451–467

Flato GM, Hibler WD (1992) Modeling pack ice as a cavitating fluid. J Phys Oceanogr 22: 626–651

Gordon HB, O'Farrell SP (1997) Transient climate change in the CSIRO coupled model with dynamic sea ice. Mon Weather Rev 125: 875–907

Gordon C, Cooper C, Senior CA, Banks HT, Gregory JM, Johns TC, Mitchell JFB, Wood RA (2000) The simulation of SST, sea ice extents and ocean heat transports in a version of the Hadley Centre coupled model without flux adjustments. Clim Dyn 16: 147–168

Hunke EC, Dukowicz JK (1997) An elastic-viscous-plastic model for sea ice dynamics. J Phys Oceanogr 27: 1849–1867

Ingram WJ, Wilson CA, Mitchell JFB (1989) Modeling climate change: an assessment of sea ice and the surface albedo feedbacks. J Geophys Res 94: 8609–8622

IPCC, Climate Change (1995) The science of climate change. Cambridge University Press, Cambridge, UK, pp 572

IPCC, Climate Change (2001) The scientific basis. Contribution of Working Group 1 to the Third Assessment Report of the Intergovernmental Panel on Climate Change. In: Houghton JT, Ding Y, Griggs DJ, Noguer M, van der Linden PJ, Dai X,

Maskell K, Johnson CA (eds) Cambridge University Press, Cambridge, UK pp 881

Johns TC (1996) A description of the Second Hadley Centre Coupled Model (HadCM2). Climate Research Technical Note 71, Hadley Centre, United Kingdom Meteorological Office, Bracknell Berkshire RG12 2SY, United Kingdom, pp 19

Johns TC, Carnell RE, Crossley JF, Gregory JM, Mitchell JFB, Senior CA, Tett SFB, Wood RA (1997) The second Hadley Centre coupled ocean–atmosphere GCM: model description, spinup and validation. Clim Dyn 13: 103–134

Manabe S, Stouffer RJ (1980) Sensitivity of a global climate model to an increase of $CO_2$ concentration in the atmosphere. J Geophys Res 85: 5529–5554

Manabe S, Stouffer RJ, Spelman MJ, Bryan K (1991) Transient responses of a coupled ocean–atmosphere model to gradual changes of atmospheric $CO_2$. Part I: annual mean response. J Clim 4: 785–818

Meehl GA, Collins WD, Boville BA, Kiehl JT, Wigley TML, Arblaster JM (2000a) Response of the NCAR climate system model to increase $CO_2$ and the role of physical processes. J Clim 13: 1879–1898

Meehl GA, Boer GJ, Covey C, Latif M, Stouffer RJ (2000b) Coupled Model Intercomparison Project. Bull Am Meterol Soc 81: 313–318

O'Farrell (1998) Investigation of the dynamic sea ice component of a coupled atmosphere–sea ice general circulation model. J Geophys Res 103: 15,751–15,782

Power SB, Tseitkin F, Colman RA, Sulaiman A (1998) A coupled general circulation model for seasonal prediction and climate change research. BMRC Research Report 66, Bureau of Meteorology, Australia

Rind D, Healy R, Parkinson C, Martinson D (1995) The role of sea ice in $2\times CO_2$ climate model sensitivity. Part I: the total influence of sea ice thickness and extent. J Clim 8: 449–463

Rind D, Healy R, Parkinson C, Martinson D (1997) The role of sea ice in $2\times CO_2$ climate model sensitivity. Part II: hemispheric dependencies. Geophys Res Lett 21: 1491–1494

Russell GL, Miller JR, Rind D (1995) A coupled atmosphere–ocean model for transient climate change studies. Atmos-Ocean 33: 683–730

Shine KP, Henderson-Sellers A, Barry RG (1984) Albedo-climate feedback: the importance of cloud and cryosphere variability. In: Berger AL, Nicolis C (eds) New perspectives in climate modeling. Elsevier, Amsterdam, pp 135–155

Tokioka T, Noda A, Kitoh A, Nikaidou Y, Nakagawa S, Motoi T, Yukimoto S, Takata K (1996) A transient $CO_2$ experiment with the MRI CGCM: Annual mean response. CGER's Supercomputer Monograph Report Vol 2, CGER-IO22-96, ISSN 1341-4356, Center for Global Environmental Research, National Institute for Environmental Studies, Environment Agency of Japan, Ibaraki, Japan, pp 86

Washington WM, Meehl GA (1996) High-latitude climate change in a global coupled ocean–atmosphere–sea ice model with increased atmospheric $CO_2$. J Geophys Res 101: 12,795–12,801

Washington WM, Weatherly JW, Meehl GA, Semtner AJ, Bettge TW, Craig AP, Strand WG, Arblaster J, Wayland VB, James R, Zhang Y (2000) Parallel climate model (PCM) control and transient simulations. Clim Dyn 16: 755–774

Weatherly JW, Briegleb BP, Large WG, Maslanik JA (1998) Sea ice and polar climate in the NCAR CSM. J Clim 11: 1472–1486

Weatherly JW, Zhang Y (2001) The response of the polar regions to increased $CO_2$ in a global climate model with elastic-viscous-plastic sea ice. J Clim 14: 268–283

Wetherald RT, Manabe S (1988) Cloud feedback processes in a general circulation model. J Atmos Sci 45: 1297–1415